Contents lists available at ScienceDirect

Arabian Journal of Chemistry

journal homepage: www.ksu.edu.sa

Original article

Using red mud to prepare the iron-bearing catalyst for the efficient degradation of phenol in the Fenton-like process

Hongliang Chen [a,b,*], Qian Long [a], Yutao Zhang [a], Haihong Yang [a], Jiancheng Shu [b]

[a] College of Chemistry and Chemical Engineering, Anshun University, Anshun, Guizhou 561000, People's Republic of China
[b] Key Laboratory of Solid Waste Treatment and Resource Recycle (SWUST), Ministry of Education, Southwest University of Science and Technology, 59 Qinglong Road, Mianyang 621010, People's Republic of China

ARTICLE INFO

Keywords:
Iron-bearing catalyst
Ascorbic acid
Ferrous polymetallic oxides
Phenol pollution
Scavenging experiment
Degradation pathway

ABSTRACT

Phenol pollution is widely environmental and health problems that require new insights and urgent attention. A iron-bearing catalyst (FRM/2%A) was prepared with red mud by HCl dissolution, ascorbic acid reducing and precipitation of filter liquor, and activated H_2O_2 to degrade the phenol in synthetic wastewater. Results show that FRM/2%A had the highest degradation efficiency (99.3 %) in the reaction time of 5 min among investigative samples, due to the production of ferrous polymetallic oxides on the catalyst and the formation of mesoscopic particles and microcellular structures. The optimal conditions were 1 g/L of catalyst dosage, 5 mM of H_2O_2 concentration, 3–6 of initial pH and 100 mg/L of initial concentration of phenol in the FRM/2%A/H_2O_2 system. The degradation data fit into the pseudo-first-order kinetics model and the reaction rate constant (k) of FRM/2% A was 0.865 min^{-1}. The removal efficiency (77 %) of COD below the value (99.3 %) of phenol degradation implied the intermediates generating during the phenol degradation. The possible degradation pathway was proposed as phenol → catechol → benzoquinone → muconic acid → small molecular organic acids → CO_2 and H_2O. The findings suggested a new way for the synthesis of the efficient catalyst with RM and optimal operating strategies for the treatment of phenol wastewater.

1. Introduction

Red mud (RM) is an alkaline solid waste generated during the alumina production by Bayer process. Bayer process discharges 0.8–1.5 tons of RM per ton of alumina production (Wang et al., 2021b). About 120 million tons of RM are produced around the world, of which China produces about 30 million tons per year (Das and Mohanty, 2019). At present, 4 billion tons of RM have been accumulated approximately in different parts of the globe and this accumulation is still expanding with the rapid development of the alumina industry. The massively produced RM has become a serious environmental liability due to its high toxicity, strong alkalinity, complex composition and massive generation (Cho et al., 2019). The problems of RM have confounded the development of alumina production and alumina plants nowadays. Therefore, reliable strategies for RM disposal without significant environmental burdens are imminently desired. Up to now, the related researches of RM are mainly found in three fields (Wang et al., 2021b; Agrawal and Dhawan, 2021). First, RM was applied to making the construction and chemical materials (cement, concrete, glass, ceramics, geopolymers, composite materials, etc), of which the advantages were economical and large in scale to match the current production level of RM. This way has been regarded as the most effective approach to consume RM. However, valuable components of RM, such as compounds of Fe, Ti and rare earth, were generally considered unnecessary and wasteful in these building and most chemical materials. Second, RM was also applied to the environmental protection (adsorbents, catalysts, sewage treatment, etc) and soil improvement (the improvement of acid soil, the adsorption of some elements, etc), which brought a lot of economic benefits and achieved the purpose of "treat waste by waste". But their potential scale of industrial use of RM was limited. Third, the recycling of valuable elements in RM was performed. The techniques included magnetic separation, the wet method, the fire method and bio-metallurgy. The innovation points were to smelt valuable elements and make fuller use of the resources in RM. Deficiently, multitudinous researches on RM are still in the experimental stage and found themselves struggling to be employed in actual industrial production. Although much effort has

* Corresponding author at: College of Chemistry and Chemical Engineering, Anshun University, 25 Xueyuan Road, Xixiu District, Anshun, Guizhou Province, People's Republic of China.
E-mail address: chenhledu@126.com (H. Chen).

https://doi.org/10.1016/j.arabjc.2024.105797
Received 14 December 2023; Accepted 14 April 2024
Available online 16 April 2024

been devoted to simply direct applications of RM, it is still stacked abundantly in the slag gallery in recent years due to lacking deep processing, thorough and high value utilization, which occupies multitudes of invaluable lands and also results in severe pollutions to the environment (Agrawal and Dhawan, 2021). The deep process of RM with full utilization of valuable metals is not only imperative but also highly desired. Among various technical candidates, RM based catalysts have an expectable performance in the degradation of refractory organics as a result of the high content of iron oxides (Chen et al., 2022; Guo et al., 2022; An et al., 2022). RM typically consists of iron oxide, aluminum oxide, silicon dioxide and alkali or alkaline-earth metal compounds. These compounds are advantageous for application to the fast degradation of refractory organics, while realizing the utilization of wastes.

Phenol exists in the wastewater of various industries such as coking, pharmaceuticals, petrochemicals, oil refining, etc (Liu et al., 2018). This compound must be emphatically treated before the wastewater discharge because of its high toxicity. Thus, phenol is considered as the target contaminant in this study. The measures of phenol degradation have been proposed including physical methods (Gao et al., 2022), chemical oxidation (Yu et al., 2023) and biological treatment (Zhang et al., 2022). But the scale and economy of the reaction limit their development and application. Therefore, more researchers are focusing on the catalytic degradation of phenol because of its utilization of speediness, green and high efficiency. From this, seeking low cost and efficient catalysts will be the emphasis and difficulty of subsequent researches. Advanced oxidation processes (AOP), as promising approaches to mitigate increasing demands on water purification and satisfy correspondingly strict regulations, have attracted a considerable attention because of its high oxidation activity and good adaptability. Among AOP, the Fenton reaction based on the generation of hydroxyl radicals (·OH) is known as a non-selective reactivity, cheap and highly efficient way for the degradation of refractory organics (Gao et al., 2018). Its conventional version utilizes homogeneous Fe^{2+} species as a H_2O_2 activator to evolve ·OH, while involving the oxidation of Fe^{2+} to Fe^{3+}. The generation of ferric hydroxide sludge is detrimental to retain Fe^{2+}/Fe^{3+} redox cycle during the reaction and also regarded as a secondary pollution. Given this, the heterogeneous Fenton process has been developed because of its easy separation (Fenton-like reaction). While there are two main drawbacks of current heterogeneous Fenton catalysts: lower activities due to sluggish the rate of ·OH production and the poor stability of the catalysts because of serious leaching of active metals ions. Therefore, it is indispensable to develop heterogeneous Fenton-like catalysts with high activity and great durability.

In the recent decade, iron-bearing materials, including zero-valent iron, pyrite and iron oxides, have been studied for the Fenton-like reaction (Pouran et al., 2014) and had the great advantage to other materials in the specific surface area and range of pore size distribution. Iron-bearing materials were widely used as catalysts for the high cost-efficiency rate, easy reclaim ability, strong adsorbability and wide applicable pH range. The relationship between the crystalline structures of iron-bearing materials and catalytic activity has attracted the attention of researchers. The acceleration of doped manganese oxides on the catalytic performance of iron components was investigated for the phenol degradation. The results showed that the change of phase components played an important role in the improvement of catalytic performance (Wang et al., 2021a). MnO/Fe_3C encapsulated in N-doped carbon nanosheets could enhance the degradation of bisphenol A (Yang et al., 2022). Mn − Fe layered double oxides promoted the Mn/Fe redox cycle for electron transfer and contributed to a complete degradation of bisphenol A and 72.0 % of COD removal (Li et al., 2021b). In consideration of polymetallic oxides in RM and the low cost, it is a potential way to use RM as the source of iron active phases to prepare the catalysts of phenol degradation, which converts RM into valuable products. Thus, RM is chosen as the precursor of catalysts. Yet it was found that insensitive catalytic activity of raw RM was inefficient for the degradation of phenol in our previous study probably due to improper valence states of metal oxides and coated active substances. Thus, efforts are ongoing to change the phase components and structures for reinforcing the catalytic activity of RM. Acids, including HCl, HNO_3, H_2SO_4, etc, were used to increase active functional groups and microcellular structures of catalysts under appropriate conditions (Nasuha et al., 2021; Xu et al., 2021). In previous researches, RM was modified by a mass of reducing agents. Meanwhile, a larger amount of catalysts were found during the degradation of refractory organics compared with the results of this study (Chen et al., 2022; Saputra et al., 2012).

This study focused on using the filter liquor of RM via HCl and ascorbic acid disposing to make catalysts of the Fenton-like process for the efficient degradation of phenol. Compared studies on multiple RM-based AOP were carried out for the most efficient catalyst of phenol degradation. The characterizations of prepared catalysts were investigated to identify the active components by XRD, SEM-EDS, BET, ICP-OES and XPS technologies. Phenol degradation under different reaction conditions was studied to determine the optimal experimental conditions and evaluate the potential application as a H_2O_2 activator. The influences of different anions on phenol degradation, COD removal and Fe ions leaching were studied. The contribution of reactive oxygen species (ROS) and the degradation pathways were measured and proposed, respectively. The results are expected to benefit the further utilization of red mud to construct a high-performance refractory organics degradation catalyst.

2. Materials and methods

2.1. Materials

Phenol (C_6H_6O), hydrochloric acid (HCl), hydrogen peroxide (H_2O_2), *tert*-butanol ($C_4H_{10}O$) and ammonia (NH_3) were purchased from Shanghai Macklin Biochemical Co. Ltd., China. Ascorbic acid ($C_6H_8O_6$) was obtained from Xilong Scientific Co. Ltd., China. All used chemicals and reagents were analytical grade, and deionized water was throughout the whole experiment. RM, obtained from a residue storage facility of an alumina refinery plant in Anshun city, Guizhou province, China, was firstly washed using deionized water to remove soluble alkaline substances and oven-dried at 105 °C. Then the sample was crushed by a high-speed universal pulverizer (FSJ-A05N6, Bear, China) for 3 min. RM powder was sieved under 80 mesh (0.180 mm), which was denoted as WRM and collected for subsequent experiments.

2.2. Catalysts preparation

25 g WRM was added to a 1000 mL beaker with 500 mL of 2 M HCl solution, which was brought to the boil on an electric furnace (FANAI, China) for 30 min. After cooling, 1 %−4 % of ascorbic acid as a reductant were added into the mixture and stirred for 10 min. After that, let the mixture stand for 24 h at room temperature. Then, the filter liquor was gathered by filtration through a 0.45 μm membrane filter and the filter residue was removed. Whereafter, the pH of filter liquor was regulated to 4.0 by 0.5 M ammonia (Chen et al., 2022) and the precipitate was produced simultaneously. The precipitate was dried in a vacuum drying oven (DZF-6050A, LICHEN, China) at 80 °C for overnight. The precipitates with 1 %, 2 % and 4 % of ascorbic acid disposing, denoted as FRM/1%A, FRM/2%A and FRM/4%A, respectively, were collected for the degradation of phenol. WRM was treated again by HCl with 2 % of ascorbic acid under consistent conditions with FRM/2%A. After the pH of mixture was regulated to 4.0, the residue was gathered and oven-dried overnight in the vacuum oven at 80 °C (denoted as RM/2%A). WRM was treated by HCl without ascorbic acid and the mixture pH was increased to 4.0 by 0.5 M ammonia. The residue was gathered and dried overnight in the vacuum drying oven, which was denoted as RM4. The obtained samples were used as heterogeneous Fenton-like catalysts to activate H_2O_2 for the degradation of phenol

Crystalline phases of the samples were identified by X-ray diffraction

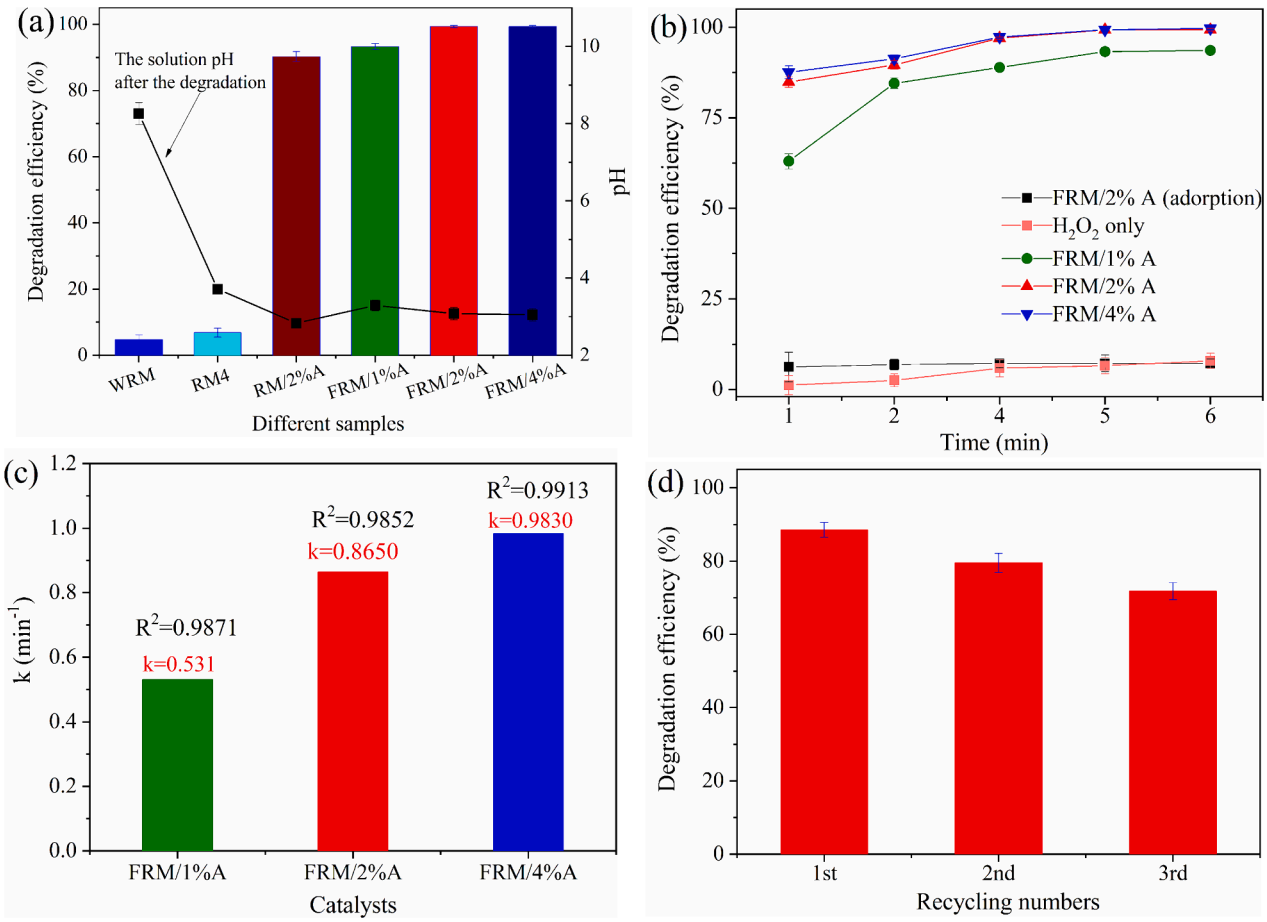

Fig. 1. Degradation of phenol by different samples within 5 min at 25 ± 1 °C (a); Change of phenol degradation with reaction time in different systems (b); The k values of pseudo-first-order kinetics of phenol degradation using FRM/x%A (x = 1, 2 and 4) (c) and the degradation efficiency of phenol in cycle tests using FRM/2% A (d).

(XRD) (X'Pert PRO, Panalytical, Holland) with Cu Kα radiation. The metal contents of WRM, RM4, RM/2%A, FRM/x%A (x = 1, 2 and 4) and FRM/2%A after the degradation were determined by an inductively coupled plasma optical emission spectrometer (ICP-OES) (VARIAN, 710ES, USA). In addition, the surface morphology and elemental mappings of samples were measured by a scanning electron microscopy (MIRA4-LMH, TESCAN, Czech Republic) equipped with an energy dispersive X-ray spectroscopy (EDS) (One Max 50, Oxford, UK). Specific surface area of samples was measured via the Brunauer-Emmett-Teller (BET) method by a nitrogen adsorption apparatus (micromeritics, ASAP2460, USA). The surface components and the chemical states of composites were analyzed on X-ray photoelectron spectroscopy (Thermo Scientific ESCALAB 250XI, USA). The zeta potential of the samples was determined at different pH levels by a Zeta potential analyzer. (Zetasize Nano ZS90, Malvern, Britain). ROS were monitored by an electron spin resonance spectroscopy (ESR) (BRUKER A300, Germany).

2.3. Investigation of catalytic activity

For the degradation experiments, batch experiments were carried out in 250 mL conical flasks with 50 mL solution of phenol at 25 ± 1 °C. Subsequently, a certain dosage of catalyst was introduced into the reaction solution. Once H_2O_2 was the reaction system, the flasks were oscillated in a water bath shaker (SHZ-82A, Changzhou Saipu, China) with a speed of 180 rpm. The pH of phenol stock solution was adjusted by 0.1 M HCl (if needed) or 0.1 M ammonia (if needed). At certain time (1–10 min), the experiments were quenched with 10 mL/L of *tert*-butanol and the cleaning solution was collected from the suspension via centrifugation for tests. The catalytic activity of different catalysts (WRM, RM4, RM/2%A and FRM/x%A (x = 1, 2 and 4)) was explored to gain the best catalyst. The influences of catalyst dosage (0.2–2 g/L), H_2O_2 concentration (2–20 mM), initial pH (2.8–8) and initial concentration of phenol (20–200 mg/L) on the degradation of phenol were investigated for the optimal conditions. The influences of inorganic ions (20–150 mg/L of Cl^-, SO_4^{2-}, NO_3^-, HCO_3^- and H_2PO_4) were inspected. The changes of COD and leaching concentration of Fe ions were detected during the phenol degradation in the different catalyst/H_2O_2 systems. ROS were identified by radical quenching tests and the ESR experiment. Intermediates of phenol degradation were identified by a liquid chromatograph spectrometer (HPLC) (Agilent1260, USA) using a UV detector set at 214 nm. To evaluate the stability and reusability of catalyst, the catalysts after the reaction were collected via the centrifugation, washed 3 times with deionized water, and dried overnight at 80 °C in a vacuum drying oven for the cycle tests. The concentration of phenol was measured by the Agilent1260 HPLC using the UV detector set at 280 nm. The mobile phase was a mixture of 40 % CH_3CN and 60 % ultrapure water. All tests were repeated three times. Subsequently, the means along with standard deviations were respectively shown in the spots and error bars of following Figures.

The degradation efficiency of phenol (φ) was calculated using Eq. (1):

$$f(\%) = 100(C_0 - C_t)/C_0 \quad (1)$$

where C_0 (mg/L) and C_t (mg/L) are the initial and time-dependent concentration of phenol, respectively.

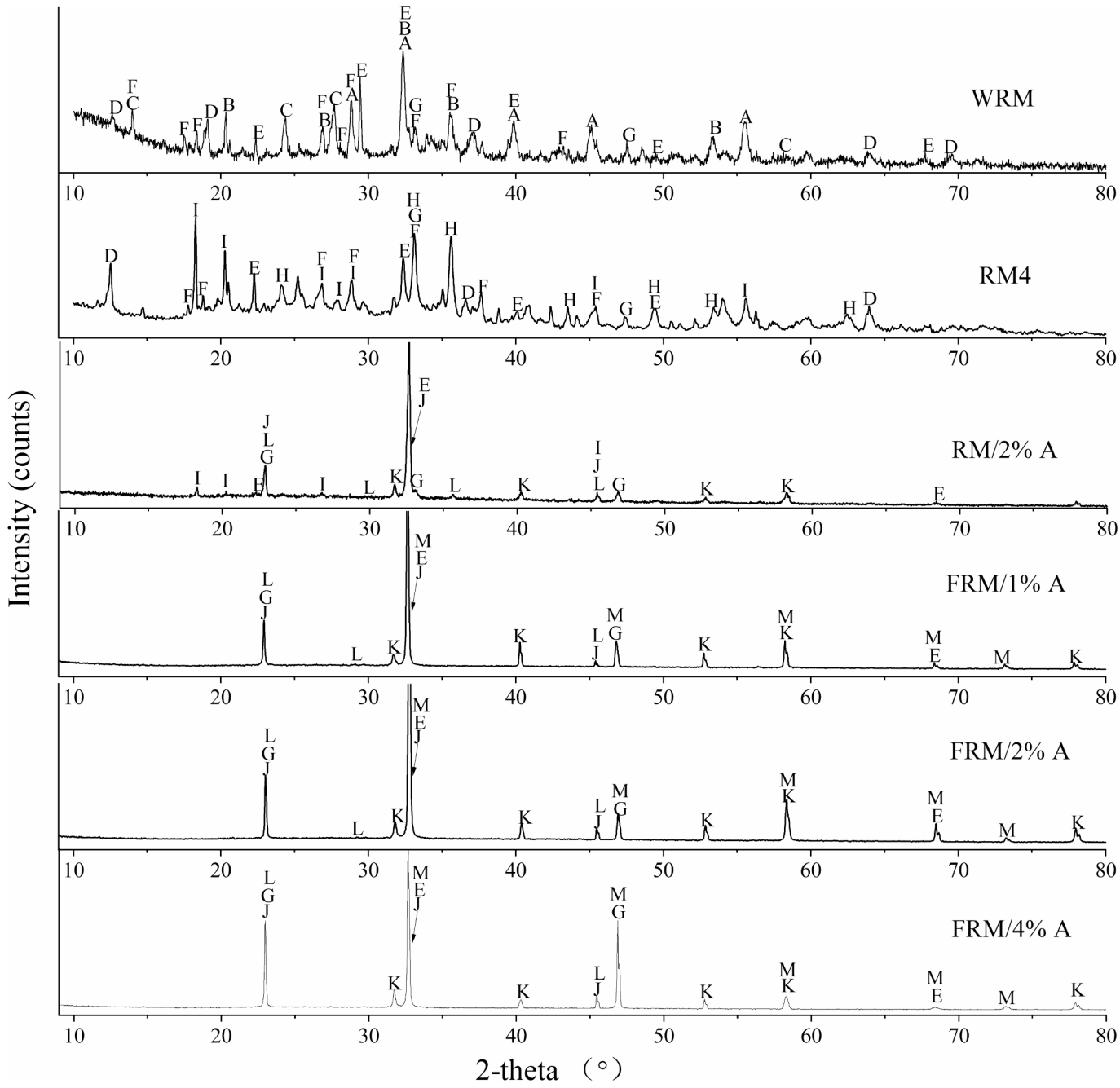

Fig. 2. X-ray diffraction patterns of WRM, RM4, RM/2%A and FRM/x%A (x = 1, 2 and 4). (A-$Ca_3Al_2(SiO_4)(OH)_8$, B-$Ca_3AlFe(SiO_4)(OH)_8$, C-$Na_8(AlSiO_4)_6(CO_3)(H_2O)_2$, D-$MnO_2$, E-$Ca_2SiO_4$, F-$FeNbO_4$, G-$CaTiO_3$, H-$Fe_2O_3$, I-$Al(OH)_3$, J-$FeMnO_3$, K-$NbFeO_3$, L-$Fe_3O_4$, M-$(La_{0.3}Sr_{0.7})FeO_3$).

3. Results and discussion

3.1. Catalytic activity

Phenol degradation results were surveyed by different catalysts under the conditions of 50 mL of 100 mg/L phenol, 5 mM H_2O_2, 1 g/L catalyst, pH 5.5 and reaction time 5 min. As shown in Fig. 1a, only 4.8 % of phenol was degraded in the WRM/H_2O_2 system, while 6.9 % of phenol was degraded in the RM4/H_2O_2 system within 5 min. The very low degradation efficiency was probably due to the improper valence states of metal oxides and the wrapped catalytic components of aggregates in WRM and RM4. As expected, the catalytic performance of modified RM was greatly enhanced via ascorbic acid reducing. 90.3 % of phenol was degraded by H_2O_2 via the activation of RM/2%A, foreboding that the reduction reaction during the catalyst preparation increased active components producing more ROS. FRM/x%A (x = 1, 2 and 4) exhibited an excellent catalytic performance for the phenol degradation. Within 5 min, about 93.3 %, 99.3 % and 99.3 % of phenol were removed by FRM/1%A, FRM/2%A and FRM/4%A, respectively. It could be seen that the solution after the catalysis degradation of phenol with the higher degradation efficiency had a lower pH, probably insinuating that acid intermediates came into being. The more the addition of ascorbic acid was, the higher the degradation efficiency was, as shown in Fig. 1b. Nevertheless, FRM/2%A and FRM/4%A contributing to the phenol degradation had little difference. In consideration of the cost of added ascorbic acid, FRM/2%A was employed as the heterogeneous catalyst for H_2O_2 activation. Fig. 1b shows that H_2O_2 alone led hardly to the phenol degradation, indicating its own poor oxidative ability. A slight

Table 1
The metal contents of different catalysts by ICP-OES analysis.

Sample	Element (%)									
	Ca	Al	Si	Na	Ti	Fe	Mn	Sr	Nb	La
WRM	12.70	11.20	0.96	4.80	2.33	7.74	0.06	0.13	0.01	0.03
RM4	5.08	12.81	1.23	0.83	3.86	11.41	0.1	0.08	0.01	0.04
RM/2%A	2.06	5.19	0.74	0.90	1.19	4.11	0.03	0.03	0.007	0.006
FRM/1%A	3.29	8.87	1.63	0.32	5.61	9.86	0.08	0.06	0.02	0.009
FRM/2%A	2.02	8.63	0.70	0.95	5.33	9.33	0.06	0.02	0.024	0.003
FRM/4%A	1.86	7.61	0.42	0.71	5.11	8.48	0.03	0.03	0.01	0.005
FRM/2%A after degradation	0.03	14.49	0.95	0.09	4.92	6.23	0.0005	0.0004	0.014	0.0002

efficiency of phenol removal (7.2 %) was seen when only FRM/2%A was added into the phenol solution, which was caused by the phenol adsorption on the surface of FRM/2%A (Gao et al., 2018). The degradation reaction fit into pseudo-first-order kinetics mode (Eq. (2)), and the reaction rate constant (k), as shown in Fig. 1c, was in the order of FRM/4%A (0.983 min^{-1}) > FRM/2%A (0.865 min^{-1}) > FRM/1%A (0.531 min^{-1}). These results indicated that an excellent synergistic effect might exist between polymetallic oxides from FRM/x%A (x = 1, 2 and 4) during H_2O_2 activation.

$$\ln(C_0/C_t) = kt \quad (2)$$

The stability and reusability of the catalyst are important factors for practical applications. Recycling tests of three times were conducted to evaluate the stability and reusability of FRM/2%A. After each run, the reaction solution was centrifuged to obtain the catalyst. Subsequently, the collected catalyst was washed three times with distilled water. Next, the catalyst was dried in the vacuum drying oven at 80 °C for overnight. Finally, 0.05 g/L of the reused catalyst was used to catalyze the degradation of the phenol. As shown in Fig. 1d, the degradation efficiency of phenol of the three cycles was 88.6 %, 79.5 % and 71.8 %, respectively. It could be noted that the phenol degradation efficiency visibly reduced during the three cycles. It could be seen that the phenol degradation efficiency after the 3rd cycle was down by 27.5 %. The results indicated that the catalytic performance of FRM/2%A was affected by repeated use, which was attributed to the dissolution of active components in FRM/2%A. Thus, the drawback of the study was the decay of the catalytic activity of 0.1 M/RM@G after manifold cycles.

3.2. Characterization of catalysts

XRD patterns of WRM, RM4, RM/2%A and FRM/x%A (x = 1, 2 and 4) are displayed in Fig. 2. The substances with potential catalytic activity covered the composites or oxides of Fe, Mn and rare earths in RM (Agrawal and Dhawan, 2021). The diffraction peaks of WRM matched highly with $Ca_3Al_2(SiO_4)(OH)_8$, $Ca_3AlFe(SiO_4)(OH)_8$, $Na_8(AlSiO_4)_6(CO_3)(H_2O)_2$, MnO_2, Ca_2SiO_4, $FeNbO_4$, $CaTiO_3$, etc. There were the diffraction peaks of Fe_2O_3 and $Al(OH)_3$ in RM4 which were probably from the decomposition of $Ca_3AlFe(SiO_4)(OH)_8$ of WRM. Although the iron contents were relatively high in WRM and RM4 by ICP-OES analysis in Table 1, improper compounds and oxides of iron led probably to the poor phenol degradation. Fe_2O_3 possessed some ability to catalyze the phenol degradation, but the efficiency wasn't high (Wang et al., 2021a).

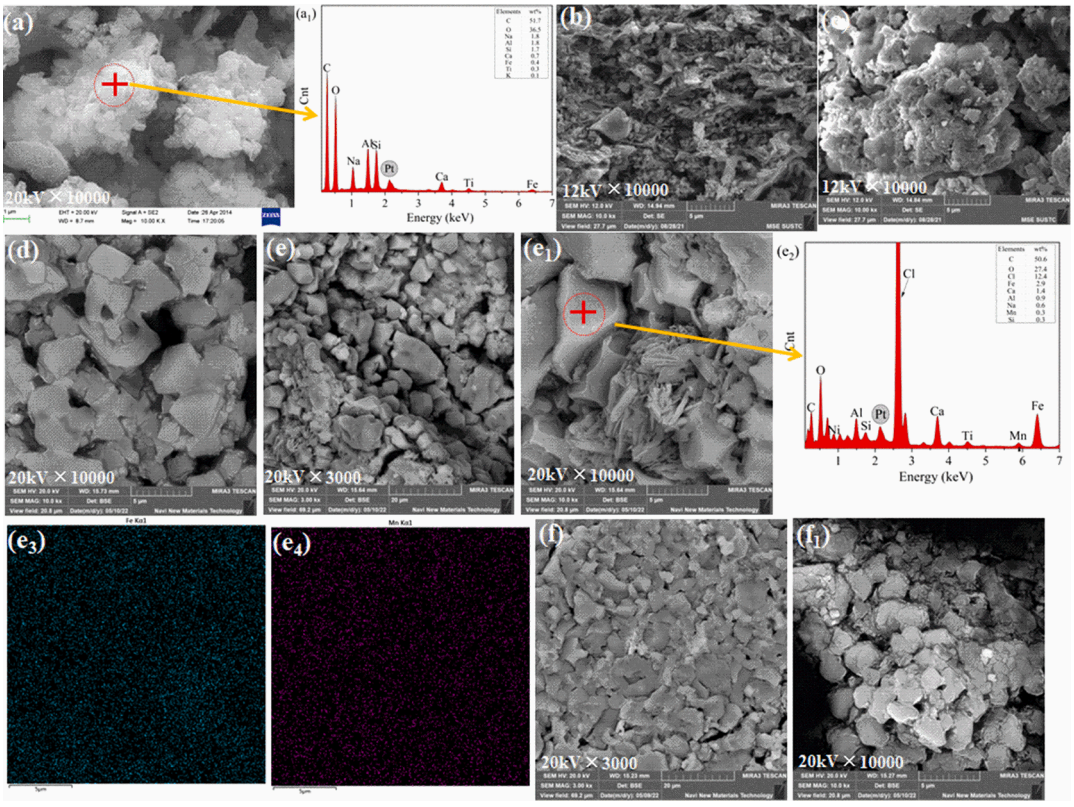

Fig. 3. Scanning electron microscopy images of WRM (a), RM4 (b), RM/2%A (c), FRM/1%A (d), FRM/2%A (e, e_1) and FRM/4%A (f, f_1); Energy dispersive X-ray spectroscopy point scans of WRM (a_1) and FRM/2%A (e_2) as well as element mapping images of Fe (e_3) and Mn (e_4) for FRM/2%A.

Table 2
Specific surface area of prepared samples.

Sample	BET surface area (m^2/g)	Langmuir surface area (m^2/g)	Total pore volume (cm^3/g)
WRM	5.80	7.59	0.003
RM4	25.47	26.04	0.013
RM/2%A	2.53	2.62	0.001
FRM/2%A	3.03	3.78	0.002

Nevertheless, $Al(OH)_3$ didn't have the ability. This was why the efficiency of RM4 was only 6.9 % for the catalytic degradation of phenol within 5 min. Characteristic peaks of $FeMnO_3$, $NdFeO_3$ and Fe_3O_4 appeared in RM/2%A, indicating that new phases formed and came most likely from the reduction of $Ca_3AlFe(SiO_4)(OH)_8$, MnO_2 and $FeNbO_4$ by ascorbic acid. $FeMnO_3$, $NdFeO_3$ and Fe_3O_4 had the excellent catalytic performance for the phenol degradation (Wang et al., 2021b), and RM/2%A gave rise to 90.3 % of phenol removal within 5 min. The reason for the restricted removal of phenol is that the lower contents of Fe, Mn and Nb in RM/2%A compared with other samples. The characteristic peaks of FRM/x%A were well indexed to the standard cards of $FeMnO_3$ (75-0894), $NdFeO_3$ (82-2421), Fe_3O_4 (75-0449) and $(La_{0.3}Sr_{0.7})FeO_3$ (82-1964). In addition, it was noted that the larger the x of FRM/x%A became, the better the crystallinity of main components was, which probably contributed to the higher efficiency of phenol degradation and indicated the synergistic effect among oxides of Fe, Mn, Nd, La and Sr. Previous studies suggested that MnO/Fe_3C, Fe_3O_4, Fe_3O_4/FeS, Fe_{1-}

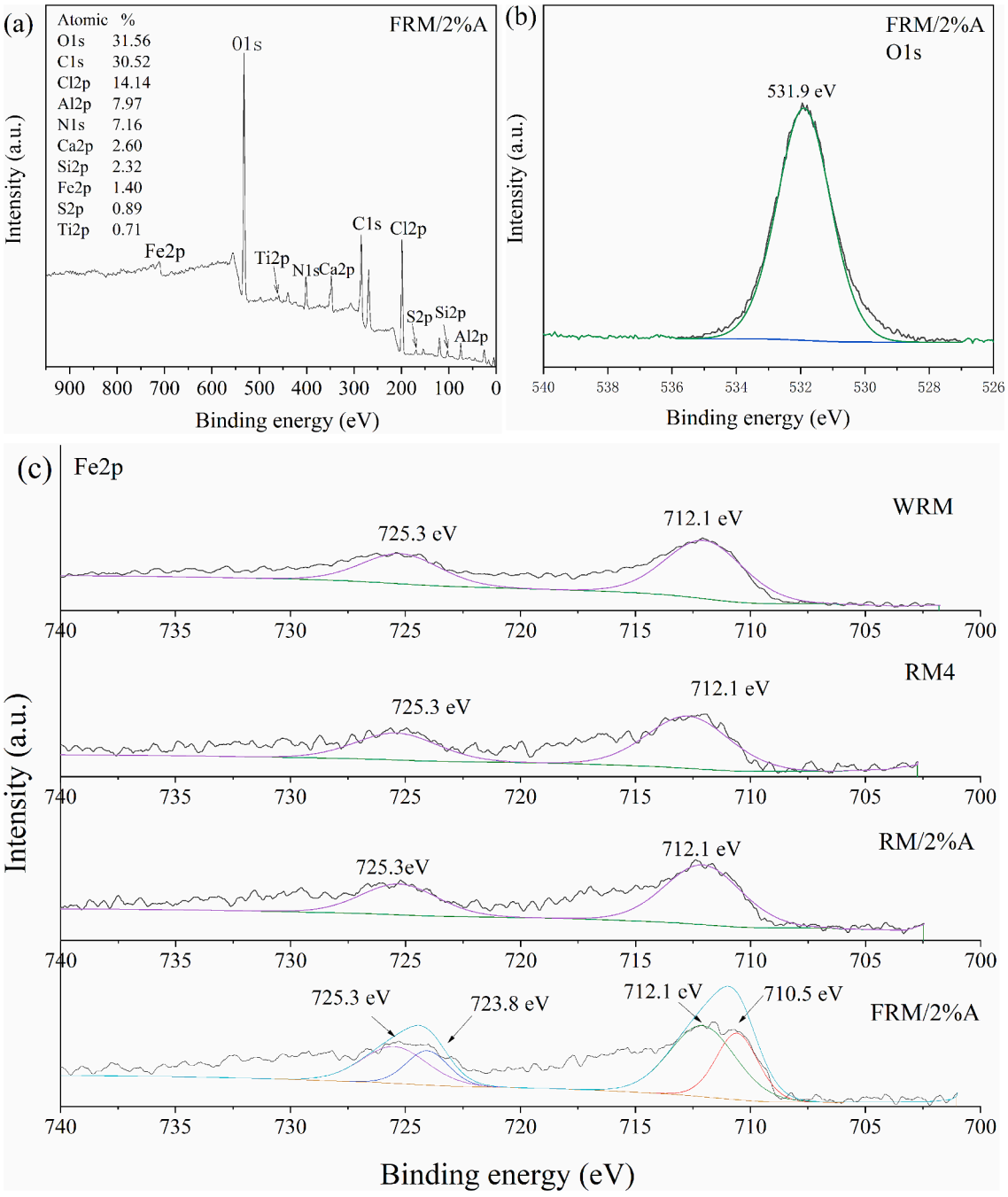

Fig. 4. Total X-ray photoelectron spectroscopy survey of FRM/2%A (a); Deconvoluted O1s spectrum of FRM/2%A (b) and Fe2p spectra of WRM, RM4, RM/2%A and FRM/2%A (c).

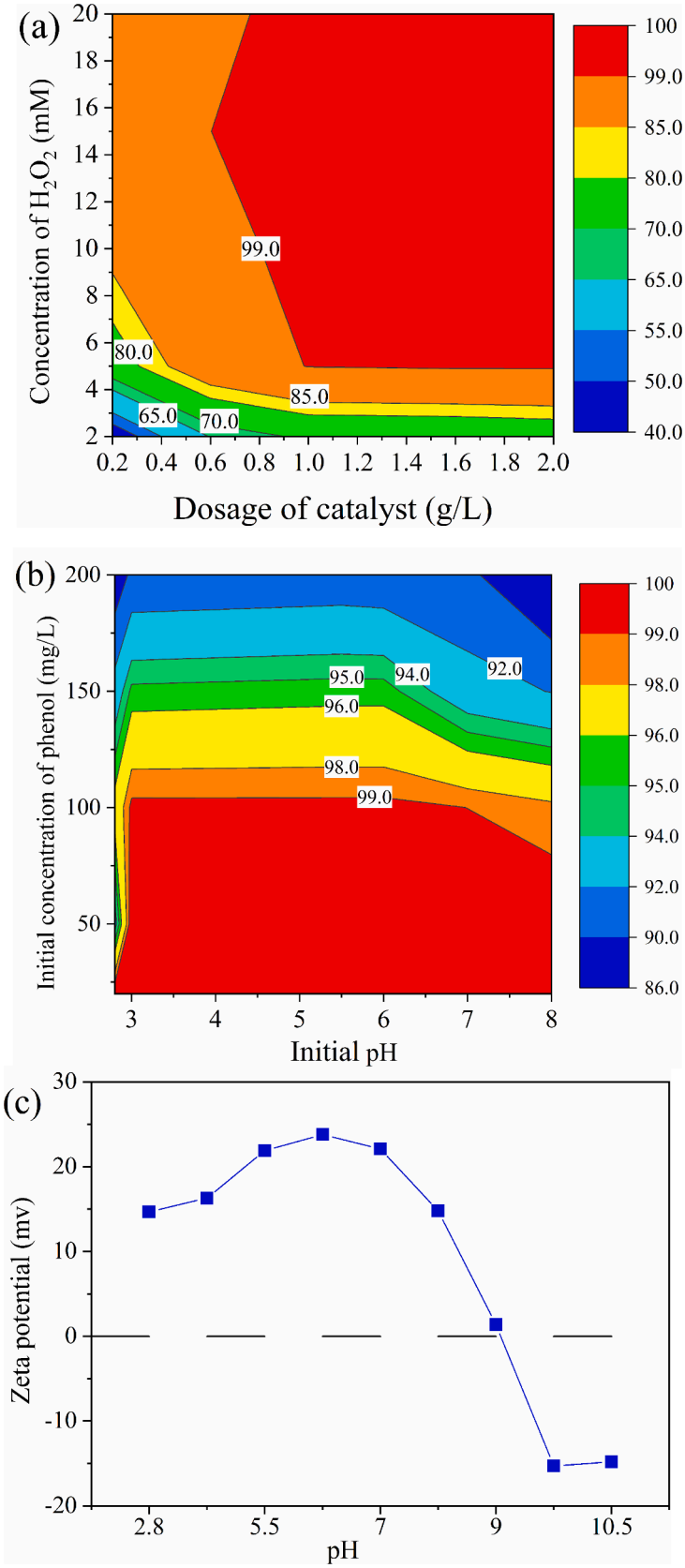

Fig. 5. Influences of FRM/2%A dosage, H_2O_2 concentration (a) and initial pH, initial concentration of phenol (b) on the degradation of phenol; Zeta potential of FRM/2%A at different pH levels (c).

Table 3
Comparison of relevant studies of phenol degradation.

Removal efficiency	Catalyst	Oxidiser	Reaction time	Experiment condition	Reference
99.3 %	FRM/2%A	H_2O_2	5 min	1 g/L catalyst, 5 mM H_2O_2, 3–6 of initial pH and 100 mg/L of initial concentration at 25 ± 1 °C	This study
82.6 %	GCM-ZnCl2	Peroxymonosulfate (PMS)	25 min	20 mg/L phenol, 2 mM PMS, 0.5 g/L catalyst and initial pH 7 at 25 °C	(Li et al., 2022)
95 %	C-MnO	H_2O_2	6 h	100 mg/L phenol, initial pH 5.8, 0.15 ml/L H_2O_2, 0.1 g/L catalyst and 333 K	(Kong et al., 2012)
97.6 %	γ-Fe_2O_3/MnO_2	PMS	80 min	35 mg/L phenol, 0.5 g/L PMS, 0.3 g/L catalyst, pH 6.4 and 30 °C	(Wang et al., 2021)
100 %	Schwertmannite	H_2O_2	5 h	100 mg/L phenol, 1 g/L catalyst, 500 mg/L H_2O_2 and initial pH 5	(Wang et al., 2013)
99.96 %	CuO_x/GAC	H_2O_2	4 min	400 W of microwave power, 100 mg/L phenol, 3 g/L catalyst, 500 mL/L H_2O_2 and initial pH 4	(Liu et al., 2018)

$_xZn_xS$, Fe/Mn loaded sludge-based carbon materials, γ-Fe_2O_3/MnO_2 nanoparticles, etc prompted oxidants degrade organic contaminants (Cheng et al., 2022; Huang et al., 2022; Li et al., 2021a; Zhao et al., 2023; Said et al., 2021). The higher content of Fe was accumulated in FRM/x%A (x = 1, 2 and 4) by ICP-OES analysis in Table 1.

The surface morphology and element compositions of the as-prepared WRM, RM4, RM/2%A and FRM/x%A (x = 1, 2 and 4) were investigated by SEM-EDS technology. According to the SEM images shown in Fig. 3, WRM showed largely and thickly agglomerated microparticles with 5.80 m^2/g BET surface area in Table 2. Whereas RM4 showed smaller and equally uneven particles with enlarged specific surface area (25.47 m^2/g), suggesting that acid etch reduced the particle size of RM and increased the honeycomb structure. RM/2%A had the larger agglomerated particles than WRM and RM4, yet exhibited the better catalytic performance for the phenol degradation compared with WRM and RM4 due to generated active components ($FeMnO_3$, $NdFeO_3$ and Fe_3O_4) on particles. As for FRM/x%A (x = 1, 2 and 4), The precipitates (FRM/1%A, FRM/2%A and FRM/4%A) from the reduced filter liquor of RM by ascorbic acid took on the larger particles and less cellular structure compared with WRM and RM4, meaning that the mesoporous structure of the samples decreased. The BET surface area of FRM/2%A was only 3.03 m^2/g and slightly more than RM/2%A in Table 2. Nevertheless, the characteristics of FRM/x%A would contribute more surface active sites for activating H_2O_2 to degrade the phenol. It was found that uniform Fe with high content was on the surface of FRM/2%A in Fig. 3e3, while uniform Mn was detected via whole map scan in Fig. 3e4. There was a higher content of Fe compared with WRM on the surface of FRM-2 %A by the point scanning, as shown in Fig. 3a1 and 3e2. The higher content of Fe on FRM/2%A probably signified more produced ferrous compounds on the surface of material, which promoted the conversion of H_2O_2 to ROS and heterogeneous Fenton catalyzing phenol degradation (Cheng et al., 2022; Huang et al., 2022).

In order to further clarify the property and the function mechanism of FRM/2%A, The surface components and the chemical states of the materials were detected by XPS technology and shown in Fig. 4. The wide survey scan of XPS spectrum of FRM/2%A indicated the presence of O1s, Fe2p, C1s, Si2p, Ti2p, etc. The O 1s XPS spectrum of FRM/2%A in Fig. 4b was used to further investigate the surface oxygen-containing groups. The binding energy of the peak was 531.9 eV and could be assigned to the surface lattice oxygen of metal − O bond (Dong et al., 2019). The high-resolution Fe 2p XPS spectra of WRM, RM4, RM/2%A and FRM/2%A were shown in Fig. 4c. The Fe 2p XPS spectra of both WRM and RM4 were deconvoluted into two peaks at 712.1 eV and 725.3 eV, ascribed to the Fe(III) 2p3/2 and Fe(III) 2p1/2, respectively. The Fe 2p XPS spectra of RM/2%A, similar to those of WRM and RM4, were distinctly divided into two peaks belonged to Fe(III) 2p3/2 and Fe (III) 2p1/2. Fe(II) 2p XPS spectra of RM/2%A were not found owing to the low content of Fe shown in Table 1. The Fe 2p XPS spectra of FRM/2%A were distinctly different from those of WRM, RM4 and RM/2%A, and deconvoluted into four peaks. Fe 2p spectra at 710.5 eV and 723.8 eV indicated the generation of Fe(II) 2p3/2 and Fe(II) 2p1/2 peaks, respectively. While, the peaks at 712.1 eV and 725.3 eV were corresponded to Fe(III) 2p3/2 and Fe(III) 2p1/2, respectively. According to the literature, the peaks 710.5 eV and 712.1 eV corresponded to Fe(II) 2p3/2 and Fe(III) 2p3/2 in Fe_3O_4 (Zhao et al., 2023). Atomic proportions of Fe(II) 2p3/2, Fe(III) 2p3/2, Fe(II) 2p1/2 and Fe(III) 2p1/2 were 24.06 %, 28.58 %, 21.65 % and 25.72 % respectively in FRM/2%A by the fitting and calculation of Thermo Avantage. The peaks of Fe 2p spectra of FRM/2%A supported probably the production of $FeMnO_3$, $NdFeO_3$, Fe_3O_4 and $(La_{0.3}Sr_{0.7})FeO_3$ by XRD analysis in Fig. 2.

3.3. Reaction parameters affecting phenol degradation

As shown in Fig. 5a, the influences of FRM/2%A dosage and H_2O_2 concentration were estimated on the degradation of phenol within 5 min under 100 mg/L phenol and initial pH 5.5 in the FRM/2%A/H_2O_2 system. When the concentration of H_2O_2 was certain, with the added dosage of FRM/2%A increased from 0.2 to 2 g/L, the degradation efficiency of phenol rose steadily. This was ascribed to more dosage of FRM/2%A providing more active sites and the more release of $\equiv Fe^{2+}$ oxides from the FRM/2%A surface for H_2O_2 activation (Liu et al., 2022b), which accelerated the production of ROS. The degradation efficiency of phenol increased with an increase of the H_2O_2 concentration at a given dosage of FRM/2%A. However, the degradation efficiency decreased slightly when the H_2O_2 concentration increased to 20 mM, ascribed to the fact that the production of ROS was quenched by excessive H_2O_2 in the FRM/2%A/H_2O_2 system (Li et al., 2021a). From the analysis of the interaction between FRM/2%A dosage and H_2O_2 concentration, the conditions were optimized at 1 g/L of catalyst dosage and 5 mM of H_2O_2 concentration.

The influences of initial pH and initial concentration of phenol on the degradation of phenol were investigated within 5 min under 1 g/L of catalyst and 5 mM of H_2O_2 in the FRM/2%A/H_2O_2 system. As shown in Fig. 5b, the solution pH had a strong effect on phenol degradation. When pH was in the range of 3–7 at the fixed initial concentration of phenol, the phenol degradation efficiency acquired the higher value and exhibited a pH-independent catalytic activity. It was well known that under the acidic condition, the surface of FRM/2%A was positively charged by Zeta potential measurement (shown in Fig. 5c) and would reinforce the affinity for H_2O_2, leading to the generation of more ROS (Yang et al., 2022). When pH of solution decreased from 3 to 2.8, the degradation of phenol decreased distinctly. This might be due to the formation of shell protonation of catalyst under low acidity, resulting in the release of hydration shell water and thereby affecting the reaction between the catalyst and H_2O_2 (Zhang et al., 2008). When the pH increased from 7 to 8, there was an obvious decrease in the degradation efficiency of phenol. At the alkaline condition, more hydroxyl ions existed in the solution reduced positive charges on the surface of FRM/2%A (in Fig. 5c) and the contact of H_2O_2 and FRM/2%A. Moreover, H_2O_2 would be decomposed quickly into water and oxygen molecules at

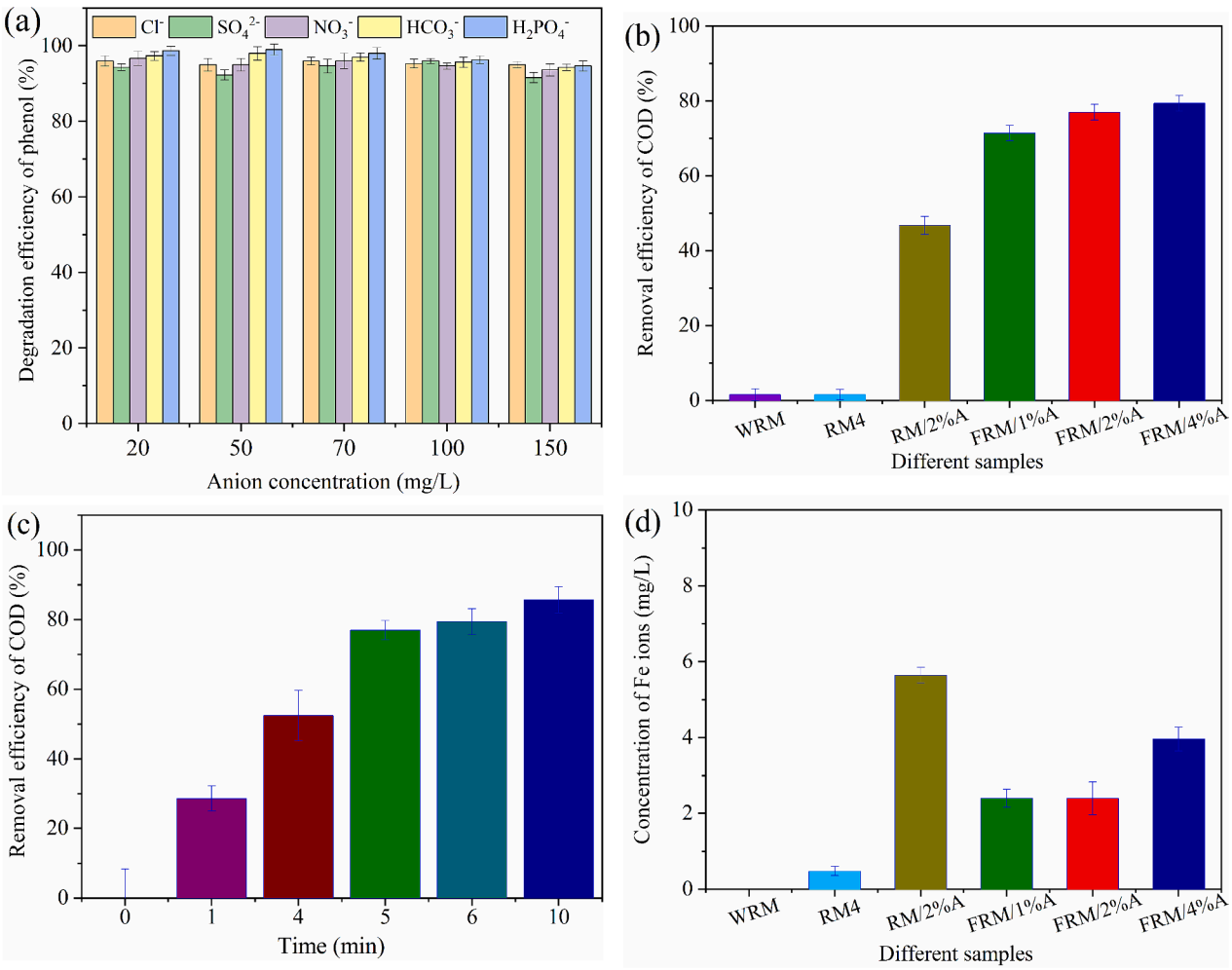

Fig. 6. Influences of different anions on the degradation of phenol (a); Removal efficiency of COD in the different catalysts/H_2O_2 systems within 5 min (b); Change of COD removal with reaction time in the FRM-2 %A /H_2O_2 system (c) and concentration of Fe ions in the different catalysts/H_2O_2 systems (d).

alkaline conditions. The degradation efficiency of phenol could decrease with increasing initial concentration at the fixed initial pH of solution. Observably, at 20 mg/L of phenol, 100 % degradation of phenol was achieved in the FRM/2%A/H_2O_2 system. As the initial concentration increased from 20 to 200 mg/L, the degradation efficiency decreased to 90.8 %. Initially at low concentration, the interaction between the catalytic sites and the molecules of H_2O_2 produced adequate ROS for the degradation of phenol. Nevertheless, the decrease of degradation efficiency for the higher concentration of phenol might be due to the inadequate rate of ROS production at the fixed dosage of catalyst. In addition, at the higher concentration, the phenol molecules probably compete with H_2O_2 for limited catalytic sites by adsorption, which brought about the decline in percentage degradation of phenol (Nasuha et al., 2021). Combining the actual phenol-contained wastewater, due to the analysis of FRM/2%A dosage and H_2O_2 concentration, the optimal conditions were 1 g/L of catalyst dosage, 5 mM of H_2O_2 concentration, 3–6 of initial pH and 100 mg/L of initial concentration of phenol. The degradation efficiency of phenol was 99.3 % under the optimal conditions. This study had an advantage compared with experiment conditions of relevant studies of phenol degradation shown in Table 3. This finding suggested a new way for the synthesis of the efficient catalyst with RM and optimal operating strategies for the treatment of phenol wastewater.

The influences of different anions, including Cl^-, SO_4^{2-}, NO_3^-, HCO_3^- and $H_2PO_4^-$, on the degradation of phenol in the FRM/2%A/H_2O_2 system are shown in Fig. 6(a). We chose Cl^-, SO_4^{2-}, NO_3^-, HCO_3^- and $H_2PO_4^-$ as the co-existing inorganic ions refering to contaminants in industrial semi-coking wastewater (Wang et al., 2022a). The degradation efficiency of phenol of the highest concentration (150 mg/L) was slightly larger than that of the lowest concentration (20 mg/L) for all investigative anions. Overall the existence of different anions would not significantly reduce the degradation efficiency of phenol, indicating that the FRM/2%A/H_2O_2 system had good environmental applicability and could be probably applied to the phenol degradation of complex industrial wastewater.

In order to explore the degree of mineralization of catalysts during phenol degradation, the chemical oxygen demand (COD) was tested under 1 g/L of catalyst, 5 mM of H_2O_2 and 50 mL of 100 mg/L phenol within 5 min. The COD manifested the total oxygen quantity of waste which is needed for the oxidation of organic molecules to CO_2 and H_2O (Mohaghegh et al., 2015). As shown in Fig. 6b, the WRM and RM4 catalysts had a very low removal efficiency of COD. However, RM/2%A had a significantly high removal efficiency of COD (46.8 %), implying that modified RM which was reduced and structured by ascorbic acid at 700 °C improved the COD removal in phenol solution. For FRM/x%A (x = 1, 2 and 4), as the value of x increased, the COD removal efficiency went up gradually. The COD removal efficiency of phenol was up to 77 % under the FRM/2%A catalyst. However, the difference of COD removal increase was not glaringly obvious as for FRM/4%A. The change of COD removal was consistent with the phenol degradation (Fig. 1a), but the removal efficiency of COD was below the degradation of phenol, which indicated the intermediates generated during the

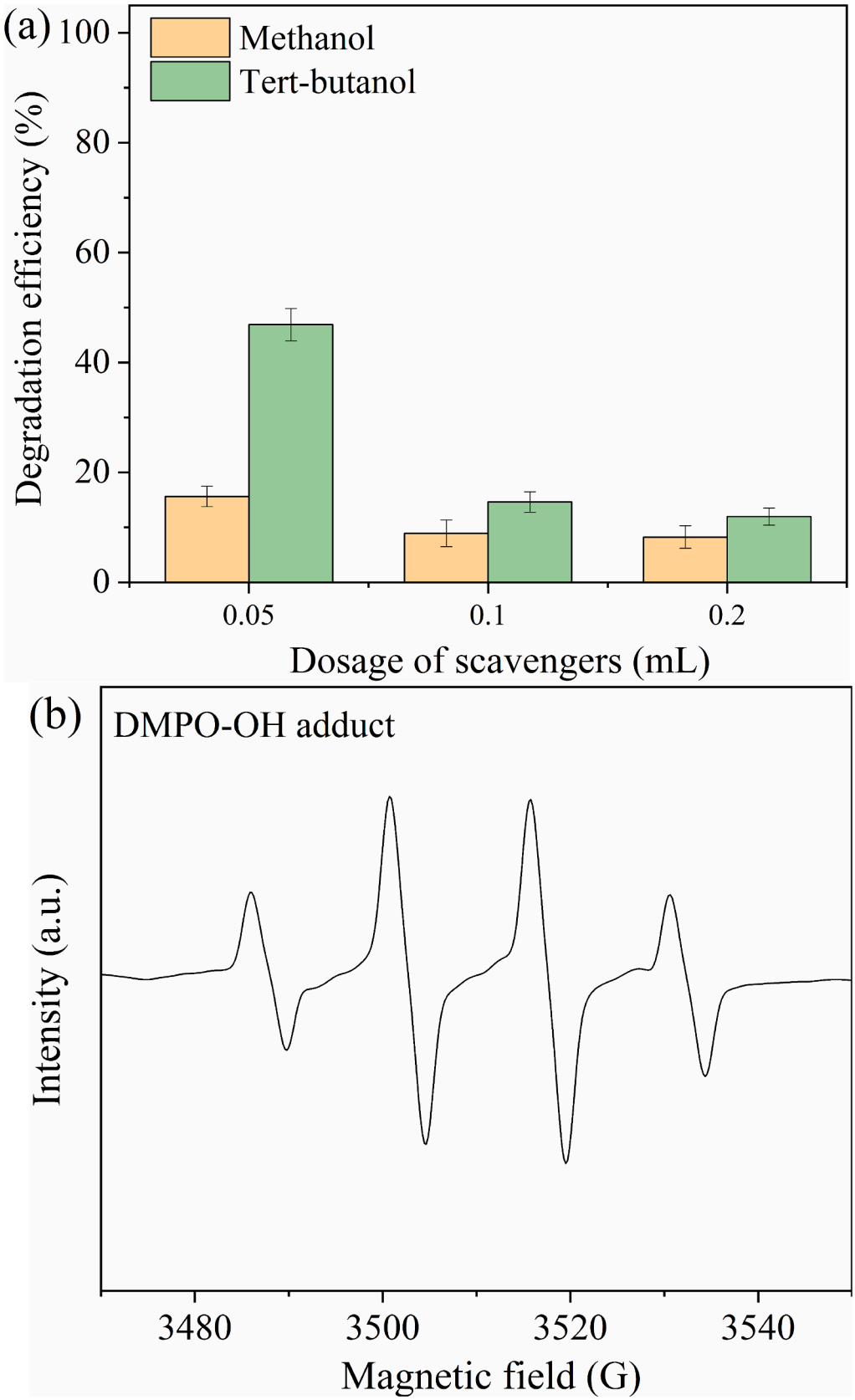

Fig. 7. Influences of different scavengers (a) on the degradation of phenol and ESR experiment (b) in the FRM/2%A/H_2O_2 system.

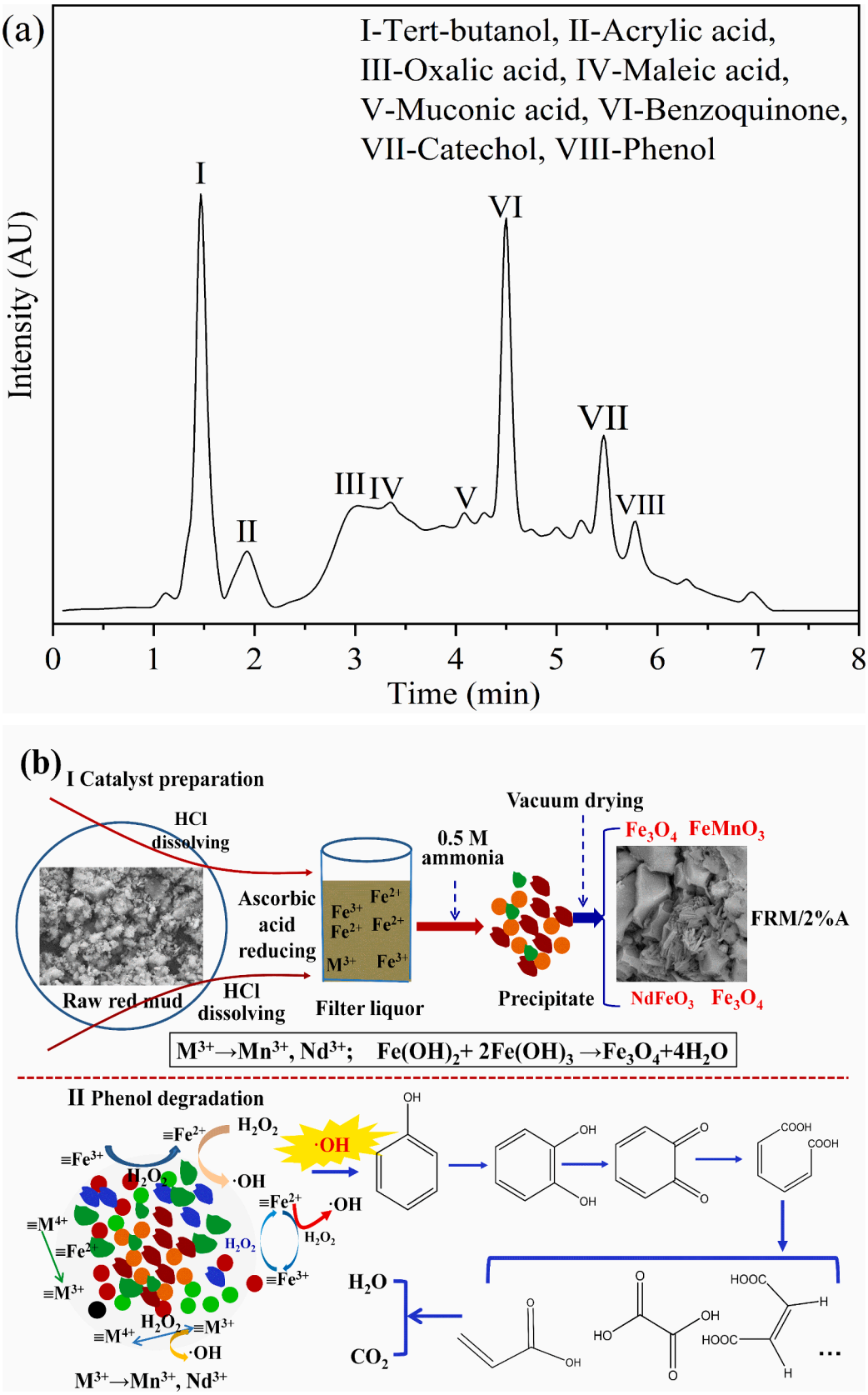

Fig. 8. HPLC pattern of intermediates during phenol degradation (a); Schematic diagrams of the change of ferrous polymetallic oxides during FRM/2%A preparation and the mechanism of phenol degradation (b).

phenol degradation. Fig. 6c showed that the COD removal efficiency of phenol was raised with the reaction time in the FRM/2%A/H_2O_2 system. The difference of COD removal augment receded obviously after 5 min.

Fe oxides were main active components activating H_2O_2 to degrade the phenol (Wang et al., 2021a; Cheng et al., 2022). Loss of Fe ions gave rise to the performance attenuation of the catalyst. The leaching characteristics of Fe ions of different catalysts during the phenol degradation were analysed and the results are shown in Fig. 6d. The leaching concentration of Fe ions of WRM and RM4 was tremendously low during the degradation, attributed to the insolubility of Fe_2O_3 in WRM and RM4. The leaching concentration of Fe ions of RM/2%A, FRM/1%A, FRM/2% A and FRM/4%A obviously increased during the degradation, probably derived from the production of Fe^{2+} compounds by ascorbic acid reducing. Leached Fe ions (2.4 mg/L) resulted in the catalytic performance of FRM/2%A attenuating in recycling tests. The Fe content of FRM/2%A was only 6.23 % after the catalytic degradation reaction by ICP-OES analysis shown in Table 1, significantly lower than that of FRM/2%A before reaction.

3.4. Identification of reactive radicals

The degradation of phenol was achieved by hydroxyl radical (·OH), which was produced from the decomposition of H_2O_2 in the system of FRM/2%A/H_2O_2 (Pang et al., 2011). To confirm the presence of ·OH, radical quenching tests were carried out and the results are illustrated in Fig. 7a. On the basis of the second-order rate constants of scavengers with ROS (Wang et al., 2022b), *tert*-butanol could be served as an scavenger of ·OH (Martha et al., 2013), and methanol could be used to scavenge $SO_4^{\cdot-}$ and ·OH (Xue et al., 2008). The degradation efficiency of phenol decreased to 15.6 % and 46.9 % within 10 min by adding 1 mL/L of *tert*-butanol and methanol, respectively. In addition, when the dosage of added *tert*-butanol and methanol increased to 4 mL/L, the degradation efficiency of phenol dropped further to 8.2 % and 11.9 %, respectively. This indicated that ·OH was the main active radicals. To identify further ·OH generated in the system of FRM/2%A/H_2O_2, DMPO-trapped EPR spectra were also used to monitor the generation of ·OH (Fig. 7b). The quartet peaks with an intensity ratio of 1:2:2:1 were the signals of DMPO-OH adduct. These results suggested that FRM/2%A could promote the decomposition of H_2O_2 to generate ·OH, while ·OH was the primary oxidative species in this Fenton-like system.

3.5. Possible degradation mechanism of phenol

Based on the results of above identification of reactive radicals, combining the reported literatures (Liu et al., 2022a; McQuillan et al., 2021), the mechanism of ·OH production was analysed as follows: $\equiv Fe^{2+}$ and $\equiv M^{3+}$ (small traces of metallic oxides, including Mn and Nd oxides) on the surface of FRM/2%A were important catalytic centers for H_2O_2 activation. They both provided electrons to H_2O_2 and initiated the decomposition of H_2O_2 to produce ·OH (Eqs. (3) and (4)). Then, the part of generated $\equiv Fe^{3+}$ and $\equiv M^{4+}$ could again react with H_2O_2 to $\equiv Fe^{2+}$ and $\equiv M^{3+}$, respectively. (Eqs. (5) and (6)). Significantly, $\equiv Fe^{2+}$ also could reduce $\equiv M^{4+}$ into $\equiv M^{3+}$, which greatly promoted the circulation of $\equiv M^{3+}/\equiv M^{4+}$ (Eq. (7)). Therefore, the redox cycles of $\equiv M^{3+}/\equiv M^{4+}$ and $\equiv Fe^{2+}/\equiv Fe^{3+}$ caused the heterogeneous chain reaction, which accelerated the formation of ·OH. In addition, phenol could be adsorbed on the surface of FRM/2%A by hydrophilic oxygen-containing groups and then degraded into a series of small molecule products by the generated ·OH, which contribute to the degradation efficiency of phenol.

$$\equiv Fe^{2+} + H_2O_2 \rightarrow \equiv Fe^{3+} + \cdot OH + OH^- \quad (3)$$

$$\equiv M^{3+}(Mn, Nd) + H_2O_2 \rightarrow \equiv M^{4+}(Mn, Nd) + \cdot OH + OH^- \quad (4)$$

$$\equiv Fe^{3+} + H_2O_2 \rightarrow \equiv Fe^{2+} + \cdot OOH + H^+ \quad (5)$$

$$\equiv M^{4+}(Mn, Nd) + H_2O_2 \rightarrow \equiv M^{3+}(Mn, Nd) + \cdot OOH + H^+ \quad (6)$$

$$\equiv M^{4+}(Mn, Nd) + \equiv Fe^{2+} \rightarrow \equiv M^{3+}(Mn, Nd) + \equiv Fe^{3+} \quad (7)$$

To realize the phenol degradation process in the FRM/2%A/H_2O_2 system, several intermediates probably existing in the reaction system are shown in Fig. 8a based on the HPLC analysis. According to the degradation products, a possible degradation pathway is proposed in Fig. 8b. ·OH radicals were generated from the Fenton-like process and played a major role in the phenol degradation. Hydroxyl group belonged to an electron donor group in the molecular of phenol and could increase the electron density of adjacent carbon atoms on the benzene ring (Li et al., 2022). ·OH radicals with strong electron affinity could selectively attack the electron rich site. Phenol was translated into catechol simultaneously. Hydroxyl group on catechol could undergo dehydrogenation and oxidation with ·OH radicals in the system. After the O–H bond was destroyed, the lone electron outside the O atom was transferred to the benzene ring carbon to form benzoquinone. Benzoquinone had the function of capturing active substances. It would be attacked easily by ·OH radicals to lead to the rupture of benzene ring and generate muconic acid. The muconic acid was further degraded into small molecular organic acids (maleic acid, oxalic acid, acrylic acid, etc) and eventually mineralized into CO_2 and H_2O.

4. Conclusions

FRM/2%A was synthesized successfully with red mud by HCl dissolution, ascorbic acid reducing and precipitation of filter liquor, which was used for activating H_2O_2 to degrade the phenol in synthetic wastewater. Ferrous polymetallic oxides, such as $FeMnO_3$, $NdFeO_3$, Fe_3O_4 and $(La_{0.3}Sr_{0.7})FeO_3$, and mesoscopic particles and microcellular structures in FRM/2%A were responsible for yielding ·OH by H_2O_2 decomposition to degrade the phenol. FRM/2%A had the highest degradation efficiency (99.3 %) among prepared samples in a pH range of 3–6 at 25 ± 1 °C. Cl^-, SO_4^{2-}, NO_3^-, HCO_3^- and H_2PO_4 anions hardly affect the degradation of phenol, implying that the FRM/2%A/H_2O_2 system had good environmental applicability. Like most heterogeneous catalysts, FRM/2%A faced the decay of the catalytic activity after manifold cycles. It is of practical significance to further anchor active components onto the RM to improve the high stability and reusability.

CRediT authorship contribution statement

Hongliang Chen: Data curation, Investigation, Methodology, Writing – original draft, Writing – review & editing. **Qian Long:** Data curation, Investigation, Visualization, Writing – review & editing. **Yutao Zhang:** Resources, Supervision, Writing – review & editing. **Haihong Yang:** Data curation, Investigation, Visualization. **Jiancheng Shu:** Conceptualization, Supervision, Writing – review & editing.

Declaration of competing interest

The authors declare that they have no known competing financial interests or personal relationships that could have appeared to influence the work reported in this paper.

Acknowledgements

This study was funded by Opening Project of Key Laboratory of Solid Waste Treatment and Resource Recycle (SWUST), Ministry of Education, Southwest University of Science and Technology (21kfgk02), the National Natural Science Foundation of China (21868001) and Key Laboratory of Agricultural Resources and Environment in High Education Institute of Guizhou Province (Qianjiaoji[2023]025).

References

Agrawal, S., Dhawan, N., 2021. Evaluation of red mud as a polymetallic source – a review. Miner. Eng. 171, 107084.

An, X., Hou, Z., Yu, Y., et al., 2022. Red mud supported on reduced graphene oxide as photo-Fenton catalysts for organic contaminant degradation. Colloid Surf. A 640, 128461.

Chen, H., Long, Q., Wei, F., et al., 2022. Enhanced Fenton removal of phenol catalyzed by a modified red mud derived from the reduction of oxalic acid and l-ascorbic acid. Environ. Sci. Pollut. R 1–11.

Cheng, A., He, Y., Liu, X., et al., 2022. Honeycomb-like biochar framework coupled with Fe_3O_4/FeS nanoparticles as efficient heterogeneous Fenton catalyst for phenol degradation. J. Environ. Sci. 136, 390–399.

Cho, D.W., Yoon, K., Ahn, Y., et al., 2019. Fabrication and environmental applications of multifunctional mixed metal-biochar composites (MMBC) from red mud and lignin wastes. J. Hazard. Mater. 374, 412–419.

Das, B., Mohanty, K., 2019. A review on advances in sustainable energy production through various catalytic processes by using catalysts derived from waste red mud. Renew. Energ. 143, 1791–1811.

Dong, Z., Zhang, Q., Chen, B.Y., et al., 2019. Oxidation of bisphenol A by persulfate via Fe_3O_4-α-MnO_2 nanoflower-like catalyst: mechanism and efficiency. Chem. Eng. J. 357, 337–347.

Gao, W., Lin, Z., Chen, H., et al., 2022. Roles of graphitization degree and surface functional groups of N-doped activated biochar for phenol adsorption. J. Anal. Appl. Pyrol. 167, 105700.

Gao, J., Liu, Y., Xia, X., et al., 2018. $Fe_{1-x}Zn_xS$ ternary solid solution as an efficient Fenton-like catalyst for ultrafast degradation of phenol. J. Hazard. Mater. 353, 393–400.

Guo, Z., Zhang, Y., Gan, S., et al., 2022. Effective degradation of COVID-19 related drugs by biochar-supported red mud catalyst activated persulfate process: Mechanism and pathway. J. Clean. Prod. 340, 130753.

Huang, X., Xiao, J., Yi, Q., et al., 2022. Construction of core-shell Fe_3O_4@ GO-CoPc photo-Fenton catalyst for superior removal of tetracycline: The role of GO in promotion of H_2O_2 to ·OH conversion. J. Environ. Manage. 308, 114613.

Kong, L., Wei, W., Zhao, Q., et al., 2012. Active coordinatively unsaturated manganese monoxide-containing mesoporous carbon catalyst in wet peroxide oxidation. Acs Catal. 2, 2577–2586.

Li, L., Deng, Y., Ai, J., et al., 2021a. Fe/Mn loaded sludge-based carbon materials catalyzed oxidation for antibiotic degradation: persulfate vs H_2O_2 as oxidant. Sep. Purif. Technol. 263, 118409.

Li, C., Wang, S., Zhang, X., et al., 2022. In-situ preparation of coal gangue-based catalytic material for efficient peroxymonosulfate activation and phenol degradation. J. Clean. Prod. 374, 133926.

Li, L., Zhang, Q., She, Y., et al., 2021b. High-efficiency degradation of bisphenol A by heterogeneous Mn–Fe layered double oxides through peroxymonosulfate activation: performance and synergetic mechanism. Sep. Purif. Technol. 270, 118770.

Liu, D., Chen, D., Hao, Z., et al., 2022a. Efficient degradation of Rhodamine B in water by $CoFe_2O_4$/H_2O_2 and $CoFe_2O_4$/PMS systems: a comparative study. Chemosphere 307, 135935.

Liu, Z., Meng, H., Zhang, H., et al., 2018. Highly efficient degradation of phenol wastewater by microwave induced H_2O_2-CuO_x/GAC catalytic oxidation process. Sep. Purif. Technol. 193, 49–57.

Liu, X., Xu, P., Fu, Q., et al., 2022b. Strong degradation of orange II by activation of peroxymonosulfate using combination of ferrous ion and zero-valent copper. Sep. Purif. Technol. 278, 119509.

Martha, S., Nashim, A., Parida, K., 2013. Facile synthesis of highly active gC_3N_4 for efficient hydrogen production under visible light. J. Mater. Chem. A 1, 7816–7824.

McQuillan, R.V., Stevens, G.W., Mumford, K.A., 2021. Assessment of the electro-Fenton pathway for the removal of naphthalene from contaminated waters in remote regions. Sci. Total Environ. 762, 143155.

Mohaghegh, N., Rahimi, E., Gholami, M., 2015. Ag_3PO_4/$BiPO_4$ p–n heterojunction nanocomposite prepared in room-temperature ionic liquid medium with improved photocatalytic activity. Mater. Sci. Semicon. Proc. 39, 506–514.

Nasuha, N., Hameed, B., Okoye, P., 2021. Dark-Fenton oxidative degradation of methylene blue and acid blue 29 dyes using sulfuric acid-activated slag of the steel-making process. J. Environ. Chem. Eng. 9, 104831.

Pang, S.Y., Jiang, J., Ma, J., 2011. Oxidation of sulfoxides and arsenic (III) in corrosion of nanoscale zero valent iron by oxygen: evidence against ferryl ions (Fe(IV)) as active intermediates in Fenton reaction. Environ. Sci. Tech. 45, 307–312.

Pouran, S.R., Raman, A.A.A., Daud, W.M.A.W., 2014. Review on the application of modified iron oxides as heterogeneous catalysts in Fenton reactions. J. Clean. Prod. 64, 24–35.

Said, K.A.M., Ismail, A.F., Karim, Z.A., et al., 2021. A review of technologies for the phenolic compounds recovery and phenol removal from wastewater. Process Saf. Environ. 151, 257–289.

Saputra, E., Muhammad, S., Sun, H., et al., 2012. Red mud and fly ash supported Co catalysts for phenol oxidation. Catal. Today. 190, 68–72.

Wang, S., Jin, H., Deng, Y., Xiao, Y., 2021b. Comprehensive utilization status of red mud in China: a critical review. J. Clean. Prod. 289, 125136.

Wang, Y., Liu, Q., Yan, L., et al., 2022a. From pollutant to valuable phenolic resin: a novel reutilization strategy of industrial semi-coking wastewater. J. Clean. Prod. 377, 134477.

Wang, W.M., Song, J., Han, X., 2013. Schwertmannite as a new Fenton-like catalyst in the oxidation of phenol by H_2O_2. J. Hazard. Mater. 262, 412–419.

Wang, Z., Wang, Z., Li, W., et al., 2022b. Performance comparison and mechanism investigation of Co3O4-modified different crystallographic MnO2 (α, β, γ, and δ) as an activator of peroxymonosulfate (PMS) for sulfisoxazole degradation. Chem. Eng J. 427, 130888.

Wang, J., Xie, T., Han, G., et al., 2021a. SiO_2 mediated templating synthesis of γ-Fe_2O_3/MnO_2 as peroxymonosulfate activator for enhanced phenol degradation dominated by singlet oxygen. Appl. Surf. Sci. 560, 149984.

Xu, Y., Hu, E., Xu, D., et al., 2021. Activation of peroxymonosulfate by bimetallic CoMn oxides loaded on coal fly ash-derived SBA-15 for efficient degradation of Rhodamine B. Sep. Purif. Technol. 274, 119081.

Xue, M., Huang, L., Wang, J.Q., et al., 2008. The direct synthesis of mesoporous structured MnO_2/TiO_2 nanocomposite: a novel visible-light active photocatalyst with large pore size. Nanotechnology 19, 185604.

Yang, T., Song, Y., Yang, Y., et al., 2022. Synergistic activation of peroxymonosulfate by MnO/Fe3C encapsulated in N-doped carbon nanosheets for the enhanced degradation of bisphenol A. J. Environ. Chem. Eng. 10, 107251.

Yu, S., Peng, Y., Shao, P., et al., 2023. Electron-transfer-based peroxymonosulfate activation on defect-rich carbon nanotubes: understanding the substituent effect on the selective oxidation of phenols. J. Hazard. Mater. 442, 130108.

Zhang, H., Ling, Z., Ma, J., et al., 2022. Biodegradability enhancement of phenolic wastewater using hydrothermal pretreatment. Bioresource Technol. 367, 128199.

Zhang, J., Zhuang, J., Gao, L., et al., 2008. Decomposing phenol by the hidden talent of ferromagnetic nanoparticles. Chemosphere 73, 1524–1528.

Zhao, L., Wan, N., Jia, Z., et al., 2023. Efficient degradation of tetracycline: Performance and mechanism study of Fe_3O_4@CF composite electrode materials applied to a non-homogeneous photo-electro-Fenton process. J. Environ. Chem. Eng. 11, 110211.